# Numerical Investigation of Integrating Electromagnetic Forming with Supercritical Fluid-Assisted Polymer Injection Molding

**M. Pirani[1,2], M. Hahn[3], H. Dardaei Joghan[3], Y. P. Korkolis[3], A. E. Tekkaya[3], S. Farahani[1,2*]**

[1] School of Mechanical and Automotive Engineering, Clemson University, USA
[2] Clemson Composites Center, Clemson University, U.S.A
[3] Institute of Forming Technology and Lightweight Components, TU Dortmund University, Germany
*Corresponding author. Email: sfaraha@clemson.edu

## Abstract

*Lightweight sheet metal-polymer components with micro- to nanocellular structures offer a unique combination of structural performance and functional properties. Using conventional manufacturing approaches requires complex and costly multi-stage manufacturing routes to realize such components. Moreover, achieving polymer foams with fine morphology is challenging due to the limitations in precise control over the current foaming technique. To address this limitation, this study explores the novel concept of integrating electromagnetic forming with supercritical fluid (SCF)-assisted polymer injection molding, called the electromagnetic forming injection foaming (EFIF) process. To investigate the feasibility of this integration, a combined numerical-analytical framework is developed using Abaqus finite element (FE) software and cell nucleation analytical models. Simulations are conducted and compared with experimental results to evaluate the influence of this integration on the electromagnetic stage. The deformation rates extracted from the Abaqus simulations are incorporated into a set of modified analytical models based on classical nucleation theory to estimate the pressure drop dynamics. This study provides a more accurate representation of cell formation within the EFIF process by coupling these pressure variations with the governing equations for nucleation and growth. The results demonstrate the feasibility of this integration and its potential to enable precise control over the SCF-assisted foaming process.*

# Keywords

Electromagnetic Forming, Supercritical Fluid-assisted Foaming, Hybrid manufacturing, Micro/Nanocellular Structures, Analytical-Numerical Modeling

# 1 Introduction

Multi-material design is typically employed to combine different material systems with complementary properties, resulting in enhanced performance beyond what a single material can offer (Tekkaya et al., 2014). One such multi-material approach is the combination of sheet metal and plastic, which can significantly reduce overall mass, part count, and production effort. This hybrid structure improves properties such as energy absorption and dimensional stability and allows for greater design flexibility and functional integration. Despite their advantages, the broader adoption of metal-polymer hybrids, especially in cost-sensitive sectors like automotive, remains limited due to long cycle times and high production costs. To overcome these challenges, integrated manufacturing processes such as polymer injection forming (PIF) present a viable solution (Hussain et al., 2012). In PIF, a metal blank is placed into a mold and shaped by the pressure of molten polymer injected using a standard injection molding machine, enabling cost-efficient and reliable production of sheet metal-plastic/composite components in one single operation (Farahani et al., 2018). Foaming can introduce new functional properties to multi-material parts by enhancing insulation, damping, and energy absorption capabilities. Supercritical fluid (SCF) assisted injection molding is an advanced technique that uses supercritical $CO_2$ or $N_2$ to produce high-performance foamed plastic parts. Once the polymer reaches a molten state in the injection molding barrel, SCF is injected and mixed with the melt to form a single-phase solution. This mixture is then injected into a mold at atmospheric pressure, causing a rapid pressure drop that triggers cell nucleation (Pirani et al., 2025). Key advantages of this method include reduced part weight, lower polymer melt viscosity, minimized shrinkage, and faster cooling times. To take advantage of these benefits in the PIF process, the concept of integrating SCF technology with the PIF process called SCF-assisted PIF (SFPIF), was introduced by Farahani et al. (2020) to realize lightweight, sheet metal-polymer components with microcellular structures. Increasing cell density and reducing cell size beyond microcellular structures can further enhance the properties of polymer foams, such as thermal insulation and strength-to-weight ratio. However, current large-scale production methods, particularly injection molding, struggle with poor process control and repeatability. To address these challenges, a novel method called electromagnetic forming injection foaming (EFIF) process has been introduced (Farahani et al., 2025). This new hybrid process combines two key innovations: first, it enhances the PIF technique by incorporating SCF technology, which helps overcome common PIF limitations, such as polymer melt shrinkage and high viscosity, by enabling SCF-assisted foaming during injection. The second innovation integrates an electromagnetic forming (EMF) stage, offering precise control over the foaming behavior and resulting in finely structured micro- to nanocellular foams. In this approach, a polymer melt, pre-mixed with dissolved SCF, is injected to fill the cavity while simultaneously forming the metal sheet against the mold's cavity. Following injection, a pulsed electromagnetic field is applied to shape the metal component further and hence induce a rapid pressure drop, triggering the foaming process in the polymer (Pirani et al., 2024). The schematic of the EFIF process is shown in **Fig. 1**.

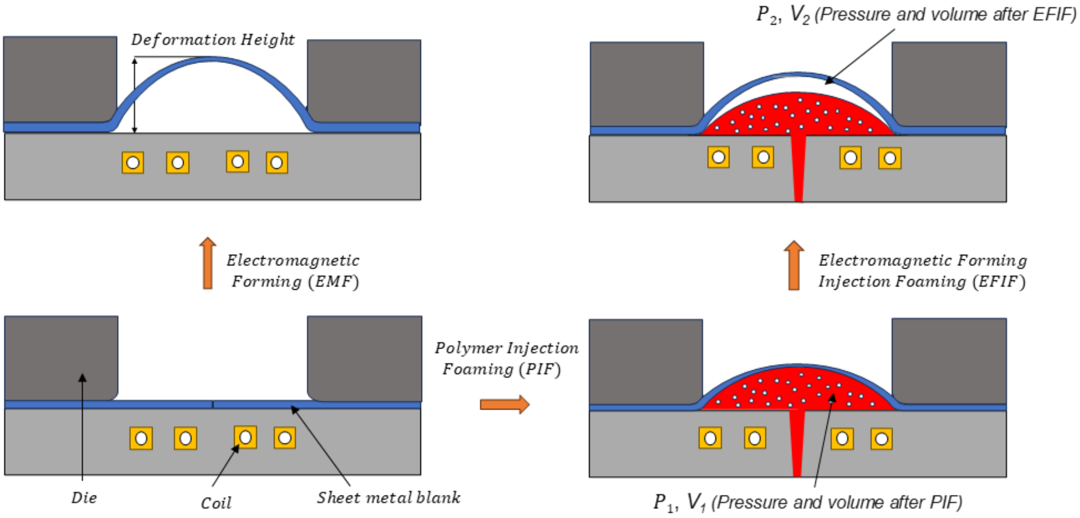

***Figure 1****: Schematic illustration of the electromagnetic forming injection foaming (EFIF) process*

## 2 Numerical-Analytical Modeling

A combined methodology involving both numerical simulation and analytical modeling was adopted to investigate the feasibility of the EFIF concept. This numerical investigation aims to evaluate the effectiveness of EMF in enhancing the foaming behavior by inducing a significant pressure drop, which in turn promotes cell nucleation within the polymer matrix. The simulation framework was implemented in Abaqus 2022 using a 2D axisymmetric dynamic explicit model and was executed in two sequential steps. The first step mimicked the simultaneous filling-forming stage of the PIF process by applying a uniform load all over the deformation zone. The second step simulated the high-speed EMF process, incorporating a varying analytical pressure field derived from magnetic field equations.

The results obtained from the simulation, particularly displacement fields and deformed volume, were extracted and used as inputs for a set of equations derived from classical heterogeneous nucleation theory.

### 2.1 Finite Element Models

To reduce computational cost and simplify the simulation setup, a 2D axisymmetric model was developed in Abaqus 2022, considering free-forming conditions for the PIF step and circular coils for the following EMF step. A circular sheet metal blank with a thickness of 1 mm was modeled as an axisymmetric, deformable shell part, while the blank holder and die were represented as axisymmetric analytical rigid bodies. Two independent reference points were assigned to the blank holder and die to facilitate the application of boundary conditions and loading constraints. The material properties of aluminum 6061 used for the blank are detailed in **Table 1** (Farahani, 2018).

| Density *(kg/m³)* | *2710* | Yield Strength *(MPa)* | *253.16* |
|---|---|---|---|
| Modulus of Elasticity *(GPa)* | *68.9* | Poisson ratio | *0.33* |

***Table 1:*** *Material properties of AA 6061 used in simulation adopted from (Farahani, 2018)*

The material behavior in this study was modeled using the rate-dependent Johnson–Cook (J–C) constitutive flow stress equation. The parameters used here are presented in **Table 2**.

| **Material** | ***A* (MPa)** | ***B* (MPa)** | ***n*** | ***C*** | ***m*** | **$T_m$ (K)** |
|---|---|---|---|---|---|---|
| *AA 6061* | *324* | *114* | *0.42* | *0.002* | *1.34* | *925* |

***Table 2***: *Johnson-Cook material model parameters (Doley et al., 2022)*

Following the assignment of material properties and assembly of the model components, the simulation was carried out using two sequential analysis steps. The first step corresponds to the PIF process and was assigned a time increment of 0.001 seconds. The second step represents the EMF phase, simulated over a shorter duration of 0.0003 seconds to capture the high-speed nature of the process. During the first step, a uniform pressure load was applied to the top surface of the blank to emulate the mechanical pre-forming. In the second step, the electromagnetic pressure was applied as an analytical load field based on the magnetic pressure distribution described by **Eq. 1**. This equation was modified to better align with the experimental data reported by (Paese et al., 2022). It predicts the pressure distribution generated by a spirally wound, flat tool coil as a function of the coil's geometric dimensions and the transient current *I* (Psyk et al., 2011).

$$p_r = \frac{\mu_0 I^2 N^2}{2\pi^2 l^2}\left[\tan^{-1}\left(\frac{a_{air}^2+r_{o,Coil}^2-r^2}{-2a_{air}r}\right)-\tan^{-1}\left(\frac{a_{air}^2+r_{i,Coil}^2-r^2}{-2a_{air}r}\right)\right]^2 \tag{1}$$

Here, *N* represents the number of coil turns, and *l* denotes the coil winding width. The term $a_{air}$ refers to the gap between the tool coil and the workpiece. The parameters $r_{\mathrm{i,Coil}}$ and $r_{\mathrm{o,Coil}}$ correspond to the inner and outer radii of the tool coil, respectively, while r indicates the radial position at which the electromagnetic pressure is evaluated and $\mu_0$ is the magnetic permeability in a vacuum. For the simulation, the parameters were set as: N = 8, *l* = 37.5 mm, $r_{\mathrm{i,Coil}}$ = 10 mm, $r_{\mathrm{o,Coil}}$ = 47.5 mm, $\mu_0 = 4\pi \times 10^{-7}\mathrm{N.A^{-2}}$, and for the maximum current *I* = 42000A, whereby its amplitude was input as an exponentially decaying sine wave approximated from the experiments. The air gap was calculated after the PIF step, and the average value was used in step 2. A friction coefficient of 0.1 was applied, and the die and blank holder were fully constrained to fix their positions throughout the simulation. For meshing the blank, an element size of 0.1 mm was chosen to ensure sufficient resolution for capturing localized deformation and stress gradients. The blank was discretized using the CAX4R element type, a 4-node bilinear axisymmetric quadrilateral element with reduced integration and compatible with explicit dynamic analysis.

## 2.2 Cell Nucleation Analytical Models

Cell nucleation plays a key role in shaping the morphology and properties of polymer foams. A rapid nucleation rate is essential to achieve high cell density, typically driven by thermodynamic instability in the gas-polymer system. This instability is often triggered by a sudden drop in pressure, which sharply reduces gas solubility. More rapid pressure drops generally lead to more cell nucleation due to the increased instability. The classical nucleation theory is a fundamental framework for modeling various nucleation mechanisms (Pirani et al., 2024). In this study, the heterogeneous nucleation model was employed to analytically calculate the nucleation rate under EFIF processing conditions, as it providing better alignment with both the simulation results and experimental observations in terms of the magnitude and nucleation behavior. The heterogeneous nucleation rate is written as:

$$N_{het} = f_1 C_1 \, exp(-\Delta G_{het}{}^{*} \, / \, kT) \tag{2}$$

where $N_{het}$ is the heterogeneous nucleation rate, $f_1$ is the frequency factor for heterogeneous nucleation, $C_1$ represents the concentration of heterogeneous nucleation sites, $k$ is Boltzmann constant, $T$ is the absolute temperature and $\Delta G_{het}{}^{*}$ is the change in Gibbs free energy for the heterogeneous nucleation, which is expressed as:

$$\Delta G_{het}{}^{*} = \frac{16\pi}{3\Delta P^2} \gamma_{bp}^3 S(\theta_w) \tag{3}$$

$\Delta P$ represents the pressure drop inside the cavity after the injection, $\gamma_{bp}$ is the surface energy at the polymer–bubble interface, and $S(\theta_w)$is the function that depends on the wetting angle between the polymer, the gas, and the second-phase particle (Xu, 2010). To apply **Eq. 2** and calculate the theoretical heterogeneous nucleation rate, it is essential to calculate the pressure drop under EFIF processing conditions. The additional deformation induced by the electromagnetic field leads to an expansion of the cavity volume. Since the injected polymer melt is incompressible, cell nucleation and growth compensate for this volume increase, thereby initiating the foaming process (Pirani et al., 2024). Consequently, the relationship between the pressure drop and cavity volume expansion can be derived using a modified form of the ideal gas law, as shown in **Eq. 4.** Where $P_1$ and $V_1$ are the pressure and deformation volume at the end of the simultaneous filling and forming stage, $P_2$ and $V_2$ are the pressure and deformation volume after applying electromagnetic forces (see Fig. 1), and $K$ is a constant. Pressure and deformation volume can be calculated from the simulation results.

$$\Delta P = P_2 - P_1 = KT \left(\frac{1}{V_2} - \frac{1}{V_1}\right) = P_1 (\frac{V_1 - V_2}{V_2}) \tag{4}$$

# 3 Experimental investigation

Experimental investigations were conducted on AA 6061 samples formed using the PIF process, with an injection volume of 25 cm³ and a thickness of 1 mm. The samples were subsequently subjected to the EMF process without applying any additional materials such as injected polymer between the coil and sheet metal to assess their effect on the final shape, the rate of volume expansion, and the rate of pressure drop which are key factors influencing the nucleation rate. The process parameters used in the experiments were identical to those applied in the simulation studies. **Fig. 2** shows the deformation height before and after applying the EM force, along with the corresponding volume increase rate resulting from the deformation.

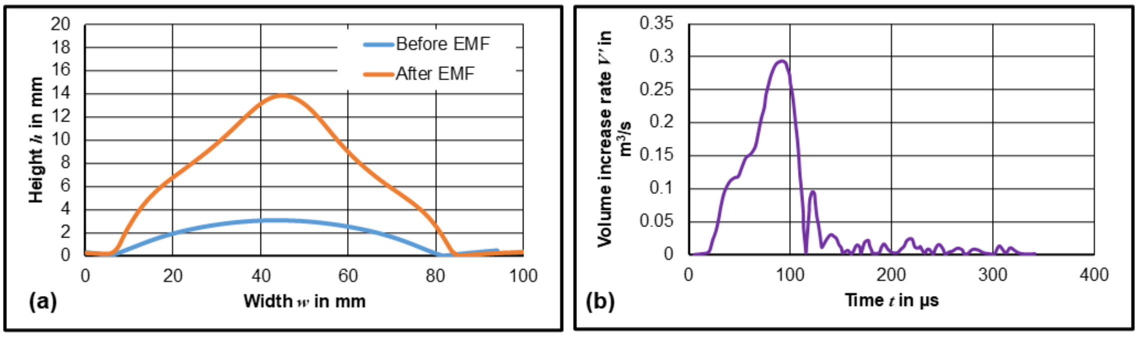

***Figure 2:*** *Experimental results for AA 6061 (a) deformation height (b) Volume increase rate*

# Results and Discussions

Based on the input parameters detailed in Section 2.1, the displacement results for each forming step and the comparative analysis between simulation and experimental results regarding the deformation height following EMF are presented in **Fig. 3**.

Using the displacement data, the deformed volume of the blank for each step was calculated and utilized in **Eq. 4** to determine the associated pressure drop. This value was then substituted into **Eq. 3** to calculate the corresponding Gibbs free energy change, which was finally placed in **Eq. 2** to calculate the heterogeneous nucleation rate. The input data used for this calculation and the results derived from the numerical simulations and the analytical cell nucleation models are listed in **Table 3**.

| $V_1$ (cm³) | $V_2$ (cm³) | $P_1$ (bar) | $P_2$ (bar) |
|---|---|---|---|
| 6.208 | 29.472 | 16 | 3.37 |
| $f_1$ (1/sec) | $\gamma_{bp}$ (dynes/cm) | $T$ (k) | $k$ (J/k) |
| 8.2 | 7.85 | 513.15 | $1.380649\times10^{-23}$ |
| $\frac{\Delta P}{\Delta t}$ (bar/sec) | $\Delta G^*_{het}$ (J) | $C_1$ (sites/cm³) | $N_{het}$ (nuclei/cm³sec) |
| $4.2\times10^{4}$ | $5.08\times10^{-21}$ | $10^{10}$ | $4\times10^{10}$ |

***Table 3:*** *Input data and calculation results*

The results demonstrate the EFIF concept's effectiveness in creating a sudden pressure drop, leading to a favorable nucleation rate essential for producing polymer foams with a micro- to nano-cellular structure. Moreover, by adjusting key EMF parameters, it is possible to control the pressure profile and optimize cell size and density. This highlights the potential of EFIF as a tunable and efficient technique for scaling the production of sheet metal-polymer parts with fine cellular structures.

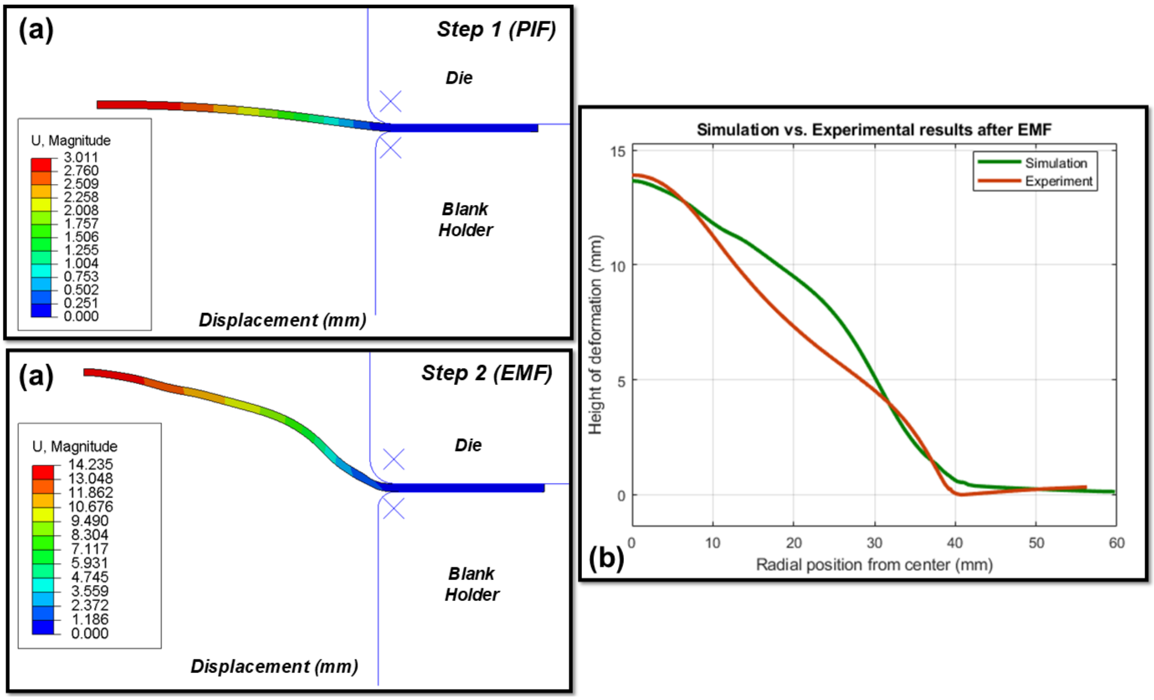

***Figure 3:*** *(a)Simulation results for each step (b)Simulation vs experiment height of deformation result*

## 4 Conclusion and Future Work

A combined numerical and analytical investigation was conducted to evaluate the feasibility of the EFIF process. Simulation results were utilized within the analytical framework to calculate the pressure drop and cell nucleation rates, providing insight into the coupling between mechanical deformation and thermodynamic conditions involved in the EFIF concept. The findings demonstrate that this novel approach has the potential for controlling SCF-assisted foaming in hybrid manufacturing processes like the PIF process, introducing a tunable and efficient technology for scaling the production of sheet metal-polymer parts with micro to nanocellular structures.

Future explorations in this direction include investigating the effects of coil geometry, current variation, and different polymers and sheet metals on the process outcome. In addition, implementing a closed-shape cavity mold will be considered to improve control over the final shape and thickness of the foamed sheet metal part. The next phase will involve the fabrication of dedicated tooling and the execution of experimental trials to validate the analytical and numerical models, along with the EFIF process for real-world industrial applications.

## References

Doley, J.K., Rajak, A.K., Kumar, R., Kore, S.D., 2022. Numerical and experimental validation for prediction of failure in electromagnetic forming of AA6061 sheet. Transactions of the Indian Institute of Metals 75, pp. 2977–2983.

Farahani, S., 2018. Polymer injection forming: A new age technology for manufacturing polymer-metal hybrids.

Farahani, S., Arezoodar, A.F., Dariani, B.M., Pilla, S., 2018. An analytical model for nonhydrostatic sheet metal bulging process by means of polymer melt pressure. Journal of Manufacturing Science and Engineering, Transactions of the ASME 140.

Farahani, S., Hahn, M., Dardaei Joghan, H., Tekkaya, A.E., 2025. A novel concept to manufacture nano/microcellular foam structures. In: Proceedings of the ASME 2024 19th International Manufacturing Science and Engineering Conference, Baltimore, USA, Paper No. MSEC2024-124138.

Farahani, S., Malmir, F., Aggarwal, D., Pilla, S., 2020a. Multi-objective optimization of sheet metal-polymer hybrids manufactured by the integrated process of deep drawing-back injection molding. SAE Technical Papers 2020-April, pp. 1–10.

Farahani, S., Pradeep, S.A., Pilla, S., 2020b. Integration concept of injection, forming and foaming: A practical approach to manufacture hybrid structures. In: Advances in Polymer Processing 2020, pp. 205–218.

Farahani, S., Yerra, V.A., Pilla, S., 2020c. Analysis of a hybrid process for manufacturing sheet metal-polymer structures using a conceptual tool design and an analytical-numerical modelling. Journal of Materials Processing Technology 279, pp. 116533.

Hussain, M.M., Trompeter, M., Witulski, J., Tekkaya, A.E., 2012. An experimental and numerical investigation on polymer melt injected sheet metal forming. Journal of Manufacturing Science and Engineering 134.

Lauwers, B., Klocke, F., Klink, A., Tekkaya, A.E., Neugebauer, R., McIntosh, D., 2014. Hybrid processes in manufacturing. CIRP Annals 63, pp. 561–583.

Paese, E., Geier, M., Homrich, R.P., Rossi, R., Rosa, P., 2022. Assessing experimental apparatus for sheet metal electromagnetic forming process analysis. Materials and Manufacturing Processes 37, pp. 1371–1383.

Pirani, M., Hahn, M., Joghan, H.D., Tekkaya, A.E., Farahani, S., 2024. On the potential of manufacturing multi-material components with micro/nanocellular structures via the hybrid process of electromagnetic forming injection foaming. Journal of Micro and Nano Science and Engineering 12, pp. 1–22.

Pirani, M., Meiabadi, M.S., Moradi, M., Enriquez, L.G., Sreenivasan, S.T., Farahani, S., 2025. On the potential of upcycling plastic wastes to carbon-capturing materials using supercritical fluid-assisted injection molding process. SAE International Journal of Sustainable Transportation, Energy, Environment, & Policy 5, pp. 13-05-03–0021.

Psyk, V., Risch, D., Kinsey, B.L., Tekkaya, A.E., Kleiner, M., 2011. Electromagnetic forming—A review. Journal of Materials Processing Technology 211, pp. 787–829.

Tekkaya, A.E., Ben Khalifa, N., Grzancic, G., Hölker, R., 2014. Forming of lightweight metal components: Need for new technologies. Procedia Engineering 81, pp. 28–37.

Xu, Jingyi, 2010. Microcellular injection molding. Wiley.